



Development of erlotinib derivatives as CIP2A-ablating agents independent of EGFR activity

Kuen-Feng Chen^{b,c,†}, Kuan-Chuan Pao^{a,†}, Jung-Chen Su^a, Yi-Chieh Chou^{b,c}, Chun-Yu Liu^{a,d}, Hui-Ju Chen^{b,c}, Jui-Wen Huang^e, InKi Kim^f, Chung-Wai Shiao^{a,*}

^a Institute of Biopharmaceutical Sciences, National Yang-Ming University, No. 155, Sec. 2, Linong Street, Taipei 112, Taiwan, ROC

^b Department of Medical Research, National Taiwan University Hospital, Taipei, Taiwan, ROC

^c National Center of Excellence for Clinical Trial and Research, National Taiwan University Hospital, Taipei, Taiwan, ROC

^d Division of Hematology and Oncology, Department of Medicine, Taipei Veterans General Hospital, Taipei, Taiwan, ROC

^e Biomedical Engineering Research Laboratories, Industrial Technology Research Institute, Hsinchu, Taiwan, ROC

^f ASAN Institute for Life Science, ASAN Medical Center, Seoul, Republic of Korea

ARTICLE INFO

Article history:

Received 30 May 2012

Revised 8 August 2012

Accepted 9 August 2012

Available online 30 August 2012

Keywords:

Erlotinib
Quinazoline
Pyrimidine
CIP2A
HCC

ABSTRACT

Cancerous inhibitor of PP2A (CIP2A) is a novel human oncoprotein that inhibits PP2A, contributing to tumor aggressiveness in various cancers. Several studies have shown that downregulation of CIP2A by small molecules reduces PP2A-dependent phosphorylation of Akt and induces cell death. Here, a series of mono- and di-substituted quinazoline and pyrimidine derivatives based on the skeleton of erlotinib (an EGFR inhibitor) were synthesized and their bioactivities against hepatocellular carcinoma were evaluated. The di-substituted quinazoline and pyrimidine derivatives were more potent inhibitors of cancer-cell proliferation than the mono-substituted derivatives. In particular, compound **1** with chloride at position 2 of quinazoline was as potent as erlotinib in inducing cell death but no inhibition for EGFR activity. Further assays confirmed a correlation between cell death, and CIP2A and Akt inhibition by these derivatives. Among all the derivatives, compounds **19** and **22** showed the most potent antiproliferative activities and the strongest inhibition of CIP2A and p-Akt expression.

© 2012 Elsevier Ltd. All rights reserved.

1. Introduction

Overexpression of cancerous inhibitor of PP2A (CIP2A) has been found in several common human cancers including acute leukemia, prostate cancer, non-small cell lung cancer, gastric cancer, head and neck cancer, colon cancer and breast cancer and has been linked to clinical aggressiveness in tumors and promotion of the malignant growth of cancer cells.^{1–7} CIP2A interacts directly with the transcription factor c-Myc and inhibits PP2A dephosphorylation of c-Myc, thereby stabilizing the oncogenic c-Myc from degradation.⁷ PP2A, a protein phosphatase, is a crucial regulator of cell proliferation by dephosphorylation of protein kinases on serine or threonine residues.⁸ PP2A is composed of three subunits which regulate substrate specificity, cellular localization and enzymatic activity. For example, PP2A dephosphorylates p-Akt at serine 473 and reduces the cell growth. Hence, the CIP2A-PP2A-Akt signaling cascade is thought to be an important survival regulator in cancers.⁵

Recently, bortezomib, a novel proteasome inhibitor, has been approved for treatment of multiple myeloma and mantle-cell lymphoma.

Bortezomib contains dipeptidyl boronic acid which is the binding site of the 26S proteasome and further inhibits the proteasome activity. Interestingly, bortezomib has also been reported to repress CIP2A expression and subsequently reduce P-Akt level and induce apoptosis in hepatocellular carcinoma (HCC).^{1,5} Therefore, development of small molecules that target CIP2A and trigger its downregulation might be a promising strategy for anti-cancer therapy.

Quinazolines have been used as a scaffold for synthesizing a variety of pharmacological compounds. For example, antagonists of human adenosine A3 receptor,⁹ inhibitors of histone lysine methyltransferase G9a,¹⁰ inhibitors of poly(ADP-ribose)polymerase,¹¹ an inhibitor of protein kinase c isotypes,¹² agonists of histamine H4 receptor¹³ and inhibitors of thymidylate synthase inhibitors.¹⁴ Amino substitutes at position 4 of quinazoline have been demonstrated to be inhibitors of epidermal growth factor receptor (EGFR) which is a receptor tyrosine kinase regulating cell proliferation.^{15–18} These agents, gefitinib, erlotinib, and lapatinib, have been approved for clinical use in cancer patients¹⁹ (Fig. 1). In addition, a combination of hydroxyheptanamide and quinazoline has been synthesized as a dual function inhibitor of histone acetyltransferase and EGFR.²⁰ It exhibited good activity against HDAC and EGFR in vitro. For the current project, we started with

* Corresponding author. Tel.: +886 2 28267930; fax: +886 2 28201866.

E-mail address: cwshiau@ym.edu.tw (C.-W. Shiao).

† These authors contributed equally to this work.

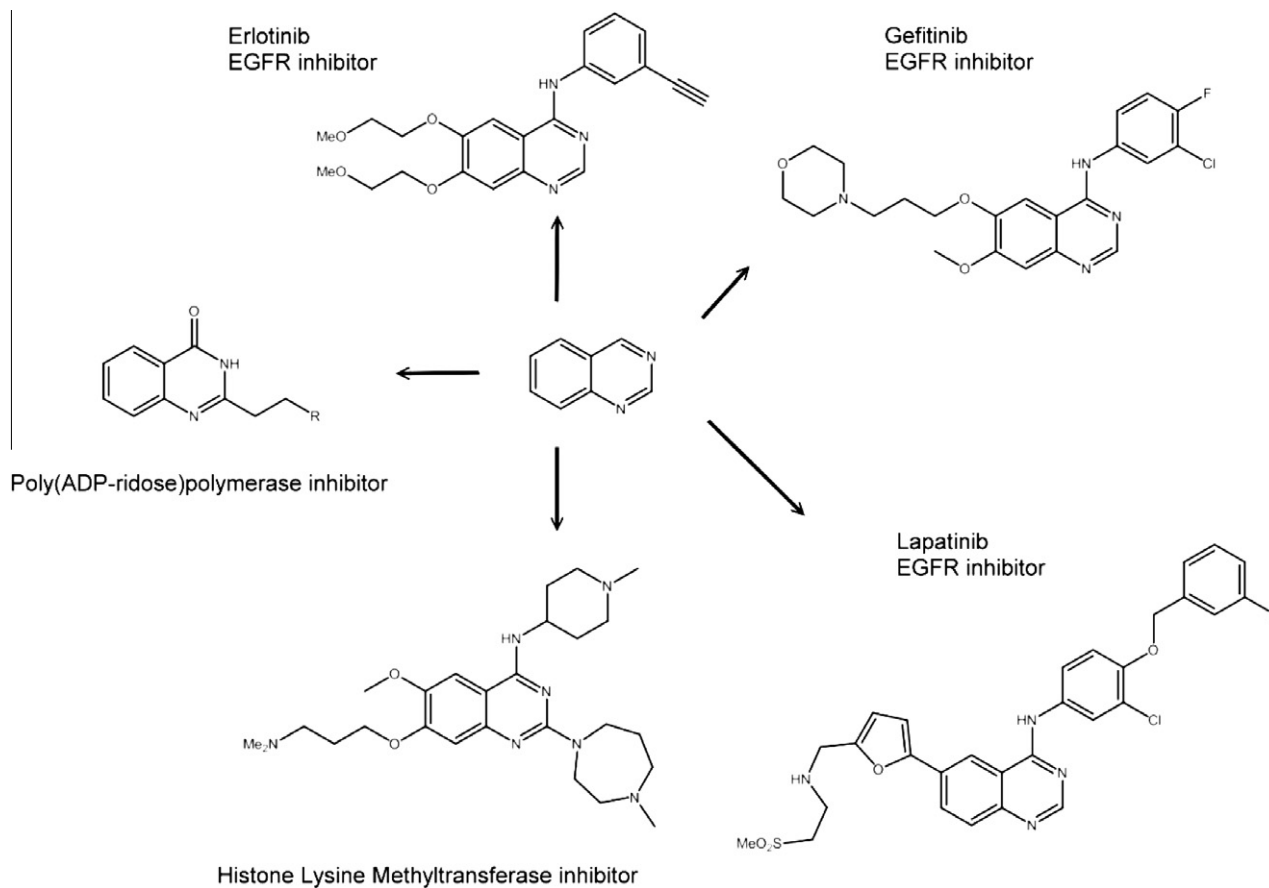


Figure 1. Inhibitors with quinazoline skeleton.

typical quinazoline-based EGFR inhibitors containing one phenylamine at position 4. Aiming to expand the structural diversity of the quinazoline substituents, we added phenylamines at position 2 of quinazoline. The inhibitory potency of these disubstituent agents against EGFR was disappointing in comparison with erlotinib, but we also found that the disubstitute-quinazoline derivatives exhibit an apoptotic effect on HCC and reduce p-Akt through repressing the expression of CIP2A. This exciting result prompted us to develop CIP2A-ablating agents.

As the disubstitute-quinazoline derivatives reduced CIP2A level, we examined their ability to induce growth inhibition in HCC cells. We investigated the structure–activity relationship (SAR) and found that these agents mediate apoptosis in association with downregulation of CIP2A in HCC cells. Western blot analyses of downstream signaling in the human HCC cell line SK-Hep-1 are also presented.

2. Chemistry

A series of quinazoline derivatives were designed and synthesized by the general procedure illustrated in Scheme 1 and the SAR of the downregulation of CIP2A by these agents was explored. Based on its core quinazoline structure, we chose commercially available dichloro-quinazoline as a starting material. A series of mono-quinazoline derivatives (compounds **1–10**) were generated with phenylamines by replacement of the chloride in the quinazoline (Table 1). We further replaced the quinazoline ring with pyrimidine and used it as a platform to carry out structural modification, which generated a series of compounds **11–17** (Table 2). Then, we replaced the other chloride from the mono-substitute

quinazolines with various phenylamines yielding compounds **18–24** (Table 3). These compounds were synthesized based on the general procedures described in Scheme 1. The inhibition of CIP2A by these compounds was analyzed by western blot assay at 20 μM of each compound.

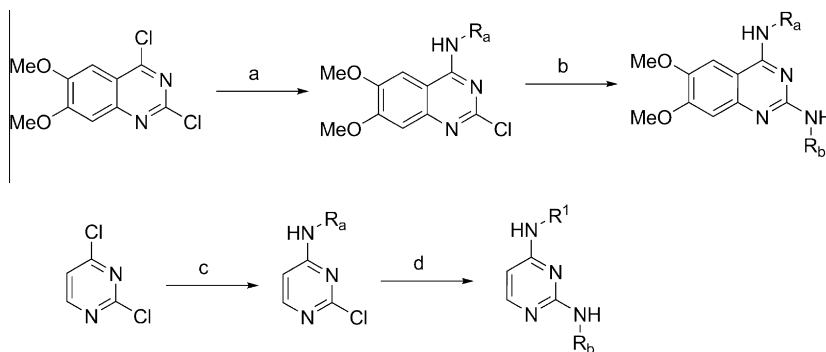
3. Biological evaluation

3.1. Development of erlotinib derivative lacking inhibition of EGFR kinase activation

An erlotinib derivative (compound **1**) was synthesized by introducing a chloride atom at the 2-position of the quinazoline ring to prevent the formation of hydrogen bonds between nitrogen of compound **1** and T790 and M793 of EGFR. A comparison of the EGFR kinase activity of erlotinib and compound **1** in PC9 cells showed that erlotinib was able to inhibit the phosphorylation of EGFR with IC_{50} at 1.36 μM but that compound **1** was devoid of EGFR kinase inhibition (Fig. 2). The result suggested that functional group connected to 2-position of quinazoline ring impeded nitrogen atom of quinazoline to act as a hydrogen acceptor and break the binding with EGFR. These findings prompt us to develop novel anticancer agents by simple introducing substituents in 2 position of quinazoline skeleton.

3.2. The structure–activity relationship of erlotinib derivative

All the new quinazoline derivatives (compounds **1–24**) were screened against a panel of SK-Hep-1 cell lines for growth-inhibitory activities. MTT (3-[4,5-dimethylthiazol-2-yl]-2,5-diphenyltetrazo-



Scheme 1. General synthesis of mono- and di-substituted quinazoline and pyrimidine derivatives. Reagents and conditions: (a) phenyl amine, HCl, *i*-PrOH; (b) phenyl amine, HCl, *i*-PrOH; (c) phenyl amine, DIPEA, *i*-PrOH; (d) phenyl amine, DIPEA, *i*-PrOH.

Table 1

Cell growth inhibitory activity of mono-substituted quinazoline derivatives as measured by MTT assay

Compd	R ¹	R ²	IC ₅₀ of cell death (μM)
1		H	7.5 ± 0.5
2		Me	12.3 ± 0.6
3		H	16.5 ± 0.8
4		H	>40
5		H	>40
6		H	8.8 ± 0.4
7		H	15.3 ± 0.6
8		H	>40
9		H	>40
10		H	19.8 ± 0.8

Table 2

Cell growth inhibitory activity of synthesized pyrimidine derivatives as measured by MTT assay

Compd	R ₁	R ₂	IC ₅₀ of cell death (μM)
11		Cl	>40
12		Cl	>40
13		Cl	>40
14		Cl	>40
15		Cl	>40
16			3.7 ± 0.2
17			13.8 ± 0.4

lium bromide) assay was used to measure growth inhibition. The compound concentrations causing 50% cell growth inhibition (IC₅₀ values) are summarized in Tables 1–3.²¹ The IC₅₀ was determined by interpolation from dose–response curves.

Compound 2, with methylation at the amine group, was equally as potent as compound 1 in inducing cell death. This implies that hydrogen donor ability is not necessary for the induction of cell death. In addition, as methylation at the amino position is known to dramatically reduce the binding ability of quinazoline with EGFR,²² compound 2 further provides a proof of concept that induction of cell death of quinazoline derivatives is independent of EGFR inhibition. When a hydroxyl group was introduced into

the phenyl ring as in compounds 4 and 8, no activity against SK-Hep1 cells was seen suggesting that hydrophobic interaction is required in this area. Compound 7 bearing a phenoxy group exhibited higher activity than compound 9 bearing a 4-cyano-phenoxy group revealing that an electron-withdrawing group is not favored for inducing cell death. Among the modified analogues (Table 1), compound 1 exhibited the most potent growth inhibitory activity. Interestingly, as the quinazoline was replaced with a pyrimidine group to generate mono and di-substituted compounds (11–17) (Table 2), no inhibitions with mono substituted at position 4 of pyrimidine derivatives 11–15 were detected in cell growth assays. However, compounds 16 and 17 with phenylamine di-substituents at positions 2, 4 in pyrimidine showed more potent anti-tumor activity than mono-substituted pyrimidine in cell growth assays. This result suggests that a phenylamine group connected to position 2 of pyrimidine plays a crucial role in cancer-cell growth inhibitory activity. Therefore, we tried to add a second phenylamine group to the quinazoline. As shown in Scheme 1, replacement of the chloride in compound 1 with a phenylamino

Table 3

Cell growth inhibitory activity of di-substituted quinazoline derivatives as measured by MTT assay

Compd	R ¹	Cell growth inhibition IC ₅₀ (μM)
18		6.8 ± 0.3
19		2.8 ± 0.1
20		7.1 ± 0.3
21		4.5 ± 0.2
22		2.8 ± 0.1
23		3.9 ± 0.2
24		14.5 ± 0.5

group resulted in di-substitute quinazoline derivatives. These derivatives showed more potent activity than mono-substituted derivatives against HCC cells (Table 3), suggesting that the second substituted component originating from quinazoline plays a significant role in the activity. In addition, compounds **19** and **22** exhibited higher potency with low IC₅₀ values (2.8 and 2.8 μM, respectively) against HCC cells whereas compound **24** only showed moderate activity, indicating that substitutions with hydrophobic properties, such as phenyloxy and benzyl groups exhibited higher

CIP2A inhibitory activity than the hydrophilic cyanophenyl groups. In addition, compound **23** showed much better inhibition than compound **24**, suggesting that the connection position of cyano-phenyl group to phenyl ring plays an important role in CIP2A inhibition.

3.3. Mechanistic validation of the mode of action of quinazoline derivatives

Quinazoline derivatives have previously been evaluated as EGFR inhibitors. However, the quinazoline derivatives we generated had very low potency against EGFR because of the second substituted group. We did, however, find that quinazoline derivatives repressed oncoprotein CIP2A expression and induced cell death. Therefore, we hypothesized that quinazoline derivatives downregulate CIP2A and p-Akt, and consequently enhance cell apoptosis. We, therefore, screened SK-Hep1 cells treated with the quinazoline derivatives at 20 μM by western blot for expression of CIP2A. As shown in Figure 3, mono-substituted pyrimidine compounds resulted in no appreciable change in CIP2A expression. Di-substituted pyrimidine and quinazoline compounds on the other hand showed a high degree of repression of CIP2A. In addition, we applied quantitative polymerase chain reaction (qPCR) assay to demonstrate that the correlation coefficient (R^2) between the IC₅₀ of CIP2A inhibition and the IC₅₀ of cell growth is 0.9519, indicating that the decreased level of CIP2A induced by these derivatives is well correlated with cell toxicity. Next, we applied potent compounds, **19** and **22**, to study whether down-regulation CIP2A and p-Akt is correlated to EGFR phosphorylation. As shown in Figure 4A, compound **19** and **22** have no inhibitory effect on EGFR. This data confirms that the second substituted-quinazoline derivatives significantly reduce the binding affinity to ATP bind domain of EGFR. We assessed CIP2A expression in response to compound **19** or erlotinib treatment in SK-Hep1 cell line. **19** reduced CIP2A expression and cell viability with a dose dependent manner and was more potent in its action than erlotinib. These result suggest that CIP2A plays an important role in regulating cell viability (Fig. 4B). Next we used three compounds, **4**, **19**, and **22**, to explore whether downregulation of CIP2A lead to suppression of p-Akt. As shown in Figure 5A, compounds **19** and **22** that showed CIP2A

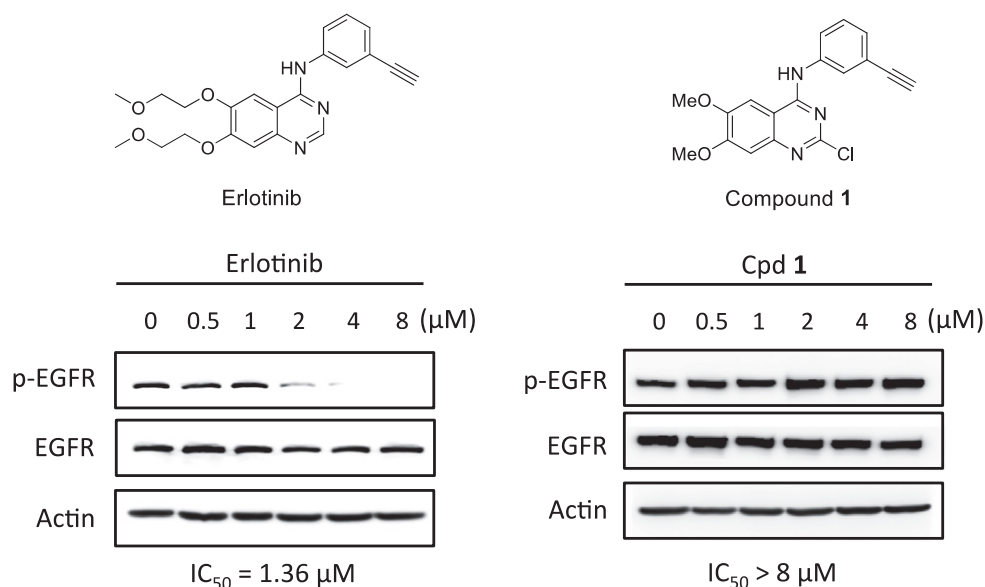


Figure 2. EGFR phosphorylation activity of erlotinib and compound **1**. PC9 cells were exposed to erlotinib or compound **1** at 0.5, 1, 2, 4, and 8 μM for 24 h and cell lysates were analyzed for EGFR phosphorylation.

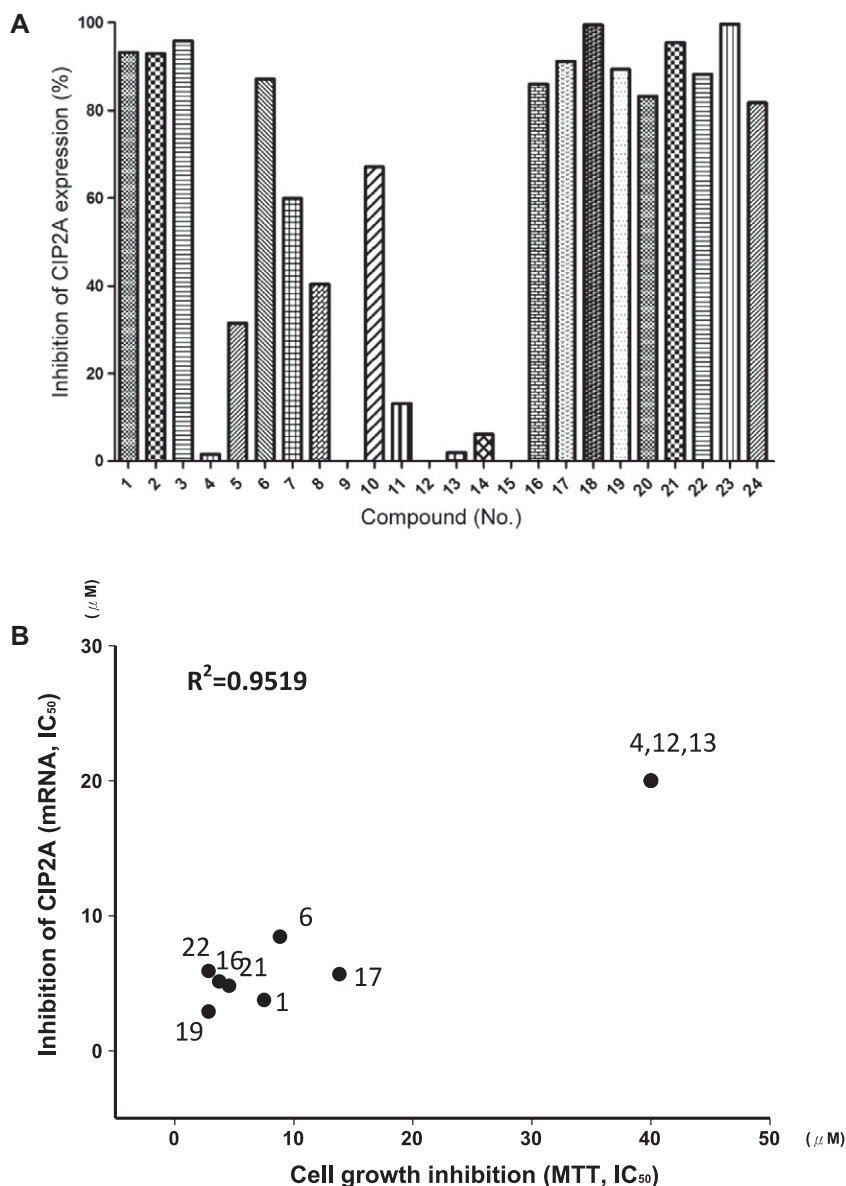


Figure 3. (A) Western blot analysis of ablative effects of CIP2A versus Actin in SK-Hep-1 cells after treatment for 24 h with compounds **1–24** at a concentration of 20 μM . (B) The IC₅₀ of CIP2A inhibition versus IC₅₀ of cell growth inhibition of quinazoline derivatives in SK-Hep-1 cells.

inhibitory activity, reduced p-Akt level, induced PARP cleavage, but compound **4** which showed no CIP2A inhibitory activity, had no effect on p-Akt and PARP. Analysis of DNA fragmentation and flow cytometry data showed that compounds **19** and **22** induced cell apoptosis, a result that is consistent with their inhibition of CIP2A expression. (Fig. 5B and C).

4. Discussion

Recent data suggest that CIP2A serves as a major regulator of cell survival by disrupting PP2A activity and subsequently increasing Akt phosphorylation. CIP2A has been shown to be protective in clinical therapy rendering it a promising drug development target.⁵ For example, a recent study demonstrated that the effect of bortezomib, a proteasome inhibitor, in HCC cells was associated with expression of CIP2A. HCC cells which have high levels of expression of CIP2A were more resistant to bortezomib treatment than HCC cells with low level of CIP2A. Therefore, agents that downregulate CIP2A can be expected to act as sensitizing drugs in patients. In this

study we focused on the structural modification of quinazoline and pyrimidine to develop a novel class of CIP2A ablative agents. Further, these quinazoline and pyrimidine-based derivatives with di-substituted phenylamines not only show great inhibition of CIP2A but also have no EGFR inhibitory activity. Presumably, the functional group at position 2 of compound **1** reduces its interaction with EGFR. Subsequent modifications of quinazoline and pyrimidine with a series of phenylamine in the 2 position resulted in decreasing CIP2A expression.

5. Conclusions

In summary, here, a series of quinazoline and pyrimidine-derived bases were synthesized and their cytotoxicity was explored with interesting SAR results. Structural modifications indicated that di-phenylamine derivatives with quinazoline and pyrimidine skeletons are required for activity. According to MTT assay, most of these derivatives had micromolar level potency against SK-Hep-1 cells. Compounds **19** and **22** showed the most potent inhibi-

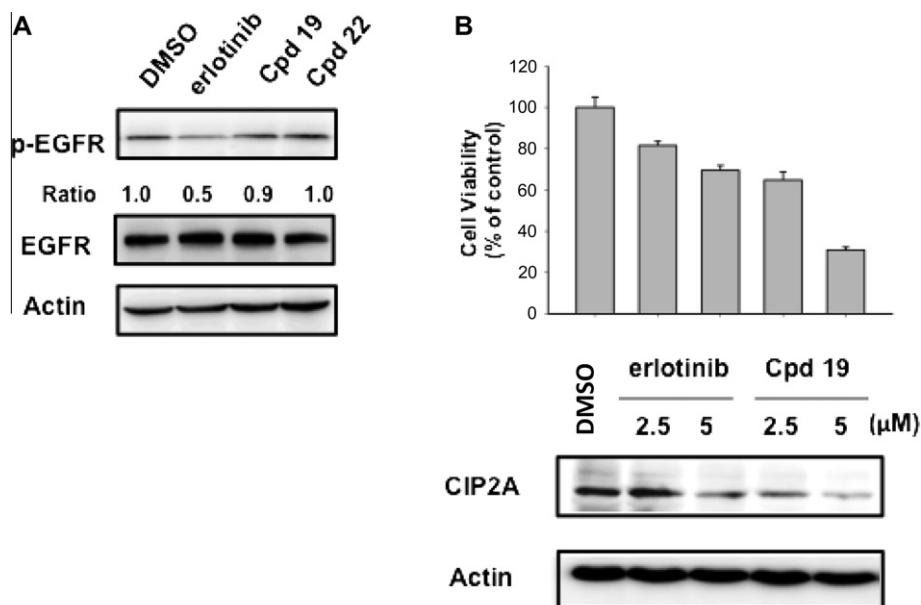


Figure 4. (A) The effect of erlotinib and compound **19** and **22** on EGFR phosphorylation activity. PC9 cells were treated with erlotinib and compound **19** and **22** at 2 μM for 24 h. (B) Compound **19** repressed CIP2A expression and inhibited cell growth as measured by MTT assay. SK-Hep-1 cells were treated with erlotinib and Compound **19** at 2.5 and 5 μM for 24 h. The cells were analyzed with western blot assay and MTT assay.

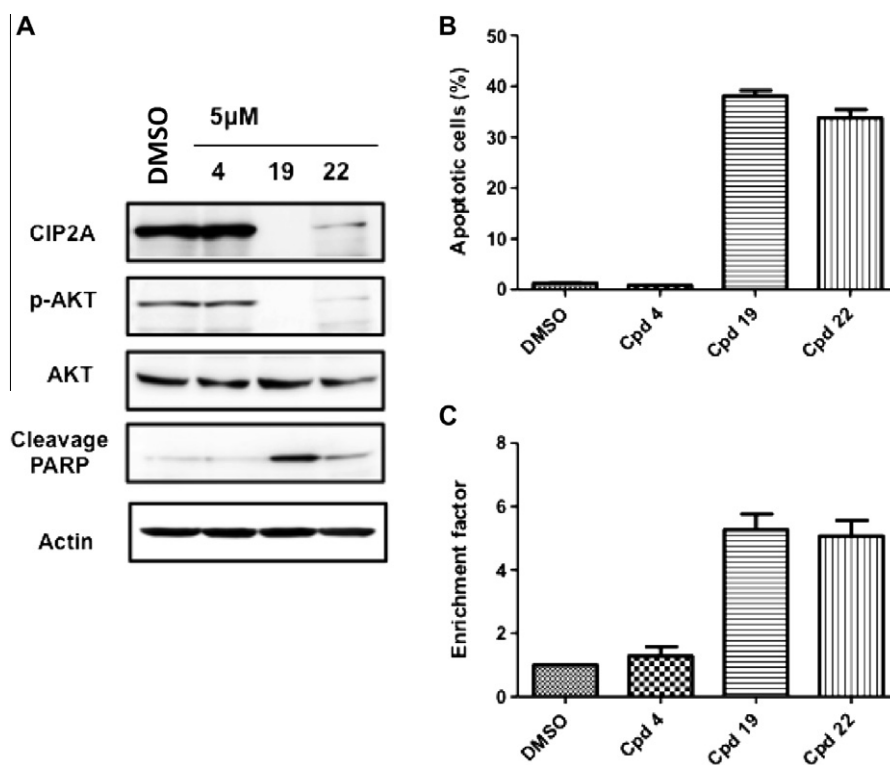


Figure 5. (A) Western blot analysis of the effects of compounds **4**, **19**, and **22**, (each at 5 μM) on CIP2A, phosphorylation of Akt, PARP and Actin, in SK-Hep-1 cells after 30 h of treatment. (B) Flow cytometry analysis of cell death induced by compounds **4**, **19**, and **22**, at 5 μM, after 24 h of treatment in SK-Hep-1 cells. Apoptotic cells were stained in potassium iodide (PI) solution and determined by flow cytometry. Columns, mean ($n = 3$); bars, SD; * $P < 0.05$. (C) Elisa analysis of cell death. Effects of compounds **4**, **19**, and **22** on DNA fragmentation in SK-Hep-1 cells. Cells were treated with compounds **4**, **19**, and **22** with indicated concentration for 24 h and DNA fragmentation was analyzed by using a cell death ELISA kit. Columns, mean ($n = 3$); bars, SD; * $P < 0.05$.

tion of CIP2A expression and cell survival activity, whereas compound **4** had no activity in either assay. Furthermore, compounds **19** and **22** reduced Akt phosphorylation after repressing CIP2A, whereas compound **4** had no activity against p-Akt and CIP2A.

These results suggest selective sensitivity in response to the different substituted functional groups in quinazoline. Moreover inhibition of CIP2A expression correlated with cytotoxicity in SK-Hep-1 cells upon drug treatment. The SARs obtained from both the

in vitro growth inhibition data and the CIP2A-Akt pathway warrant further detailed study. Testing of compounds **19** and **22** in an *in vivo* HCC model is currently being pursued.

6. Experimental section

6.1. Materials

Proton and carbon nuclear magnetic resonance (^1H and ^{13}C NMR) spectra were recorded on Bruker DPX400 (400 MHz) instruments. Chemical shifts (δ) are reported in ppm relative to the TMS peak. Peak multiplicities are expressed as follows: s, singlet; d, doublet; t, triplet; q, quartet; br s, broad singlet; m, multiplet. Reaction progress was determined by thin layer chromatography (TLC) analysis on silica gel 60 F254 plate (Merck). Chromatographic purification was carried on silica gel columns 60 (0.063–0.200 mm or 0.040–0.063 mm, Merck), basic silica gel. Commercial reagents and solvents were used without additional purification. The following abbreviations are used: CDCl_3 , deuterated chloroform; $\text{DMSO}-d_6$, dimethyl sulfoxide- d_6 ; *i*-PrOH, isopropyl alcohol; EtOAc, ethyl acetate; DMF, *N,N*-dimethylformamide; MeOH, methanol; THF, tetrahydrofuran; EtOH, ethanol; DMSO, dimethyl sulfoxide; DIPEA, diisopropylethylamine; DCM, dichloromethane. High resolution mass spectra were recorded on a Finnigan MAT 95S mass spectrometer.

6.2. Chemical synthesis

6.2.1. General procedure for the synthesis of compounds 1–10

Aniline derivative (0.8 mmol) was added to a solution of 2,4-dichloro-6,7-dimethoxyquinazoline (1.0 mmol) in isopropyl alcohol (5 ml), followed by the addition of a drop of concentrated HCl (100 μl). The resulting mixture was stirred at 60 °C for 2 h. The mixture was filtered, and the solid was washed with isopropyl alcohol then dried under vacuum to give compounds **1–10**. This procedure afforded the expected coupling product as a white or yellow solid (yield: 21–95%).

6.2.2. 2-Chloro-*N*-(3-ethynylphenyl)-6,7-dimethoxyquinazolin-4-amine (1)

^1H NMR (400 MHz, $\text{DMSO}-d_6$): δ 3.93 (s, 3H), 3.99 (s, 3H), 4.21 (s, 1H), 7.18 (s, 1H), 7.26 (d, J = 8.0 Hz, 1H), 7.43 (t, J = 8.0 Hz, 1H), 7.85 (d, J = 8.0 Hz, 1H), 7.89 (s, 1H), 7.94 (s, 1H), 10.00 (s, 1H); ^{13}C NMR (100 MHz, $\text{DMSO}-d_6$): δ 56.4, 57.2, 81.1, 83.8, 103.9, 106.6, 107.9, 122.2, 123.8, 126.0, 127.6, 129.2, 139.5, 148.1, 149.5, 154.1, 155.5, 158.4; HRMS Calcd for $\text{C}_{18}\text{H}_{14}\text{ClN}_3\text{O}_2$ (M+H): 340.0853. Found: 340.0850. Yield: 94%.

6.2.3. 2-Chloro-*N*-(3-ethynylphenyl)-6,7-dimethoxy-*N*-methylquinazolin-4-amine (2)

Methyl iodide (56 μl , 0.90 mmol) was added to a solution of **1** (61.0 mg, 0.18 mmol) and sodium hydride (60% oil suspension, 8.63 mg, 0.36 mmol) in 2 ml of DMF cooled to 0 °C. The mixture was stirred at 0 °C for 1 h, then allowed to warm to room temperature and stirred for another 1 h. The reaction mixture was washed with water, and then extracted with EtOAc. The organic phase was dried over MgSO_4 , filtered and concentrated under reduced pressure. The crude residue was purified by chromatography on a silica gel column using EtOAc/hexane as eluent (0–40%) to give compound **2** (yield: 60%). ^1H NMR (400 MHz, CDCl_3): δ 3.07 (s, 1H), 3.28 (s, 3H), 3.57 (s, 3H), 3.88 (s, 3H), 6.21 (s, 1H), 7.05 (s, 1H), 7.15 (d, J = 7.2 Hz, 1H), 7.31–7.37 (m, 3H); ^{13}C NMR (100 MHz, CDCl_3): δ 42.2, 55.2, 56.1, 78.8, 82.0, 104.8, 106.7, 108.6, 124.2, 126.7, 129.5, 130.0, 130.2, 147.5, 147.8, 150.4, 154.4, 155.0, 161.3; HRMS Calcd for $\text{C}_{19}\text{H}_{16}\text{ClN}_3\text{O}_2$ (M+H): 354.1009. Found: 354.1016.

6.2.4. 2-Chloro-*N*-(3-chlorophenyl)-6,7-dimethoxyquinazolin-4-amine (3)

^1H NMR (400 MHz, $\text{DMSO}-d_6$): δ 3.90 (s, 3H), 3.95 (s, 3H), 7.18 (s, 1H), 7.20 (d, 1H, J = 8.0 Hz), 7.44 (t, J = 8.0 Hz, 1H), 7.79 (d, J = 8.0 Hz, 1H), 7.95 (s, 1H), 7.97 (s, 1H), 10.08 (s, 1H); ^{13}C NMR (100 MHz, $\text{DMSO}-d_6$): δ 56.5, 57.1, 103.3, 106.6, 107.8, 121.3, 122.4, 124.1, 130.5, 133.1, 140.7, 148.2, 149.6, 154.1, 155.6, 158.2; HRMS Calcd for $\text{C}_{16}\text{H}_{13}\text{Cl}_2\text{N}_3\text{O}_2$ (M+H): 350.0463. Found: 350.0466. Yield: 75%.

6.2.5. 3-(2-Chloro-6,7-dimethoxyquinazolin-4-ylamino)phenol (4)

^1H NMR (400 MHz, $\text{DMSO}-d_6$): δ 3.15 (s, 1H), 3.91 (s, 3H), 3.94 (s, 3H), 6.59 (d, J = 6.8 Hz, 1H), 7.13–7.21 (m, 4H), 7.98 (s, 1H), 9.96 (s, 1H); ^{13}C NMR (100 MHz, $\text{DMSO}-d_6$): δ 56.4, 56.9, 58.5, 103.3, 106.4, 107.7, 110.6, 112.1, 114.2, 129.5, 139.8, 147.6, 149.5, 154.2, 155.4, 158.0; HRMS Calcd for $\text{C}_{16}\text{H}_{14}\text{ClN}_3\text{O}_3$ (M+H): 332.0802. Found: 332.0810. Yield: 60%.

6.2.6. 2-Chloro-*N*-(2-fluoro-5-methylphenyl)-6,7-dimethoxyquinazolin-4-amine (5)

^1H NMR (400 MHz, $\text{DMSO}-d_6$): δ 2.32 (s, 3H), 3.87 (s, 3H), 3.92 (s, 3H), 7.12–7.16 (m, 2H), 7.22 (d, J = 10.4 Hz, 1H), 7.29 (d, J = 7.6 Hz, 1H), 7.90 (s, 1H), 10.05 (s, 1H); ^{13}C NMR (100 MHz, $\text{DMSO}-d_6$): δ 20.1, 56.0, 56.3, 102.8, 105.7, 106.8, 115.61, 115.8, 124.9, 125.0, 128.1, 128.2, 128.5, 133.6, 133.7, 146.9, 149.1, 153.9, 153.9, 155.1, 156.3, 159.1; HRMS Calcd for $\text{C}_{17}\text{H}_{15}\text{ClFN}_3\text{O}_2$ (M+H): 348.0915. Found: 348.0911. Yield: 60%.

6.2.7. 2-Chloro-*N*-(4-chloro-3-(trifluoromethyl)phenyl)-6,7-dimethoxyquinazolin-4-amine (6)

^1H NMR (400 MHz, $\text{DMSO}-d_6$): δ 3.92 (s, 3H), 3.96 (s, 3H), 7.19 (s, 1H), 7.75 (d, J = 8.8 Hz, 1H), 7.99 (s, 1H), 8.19 (d, J = 8.8 Hz, 1H), 8.42 (s, 1H), 10.32 (s, 1H); ^{13}C NMR (100 MHz, $\text{DMSO}-d_6$): δ 56.0, 56.8, 102.8, 105.9, 107.3, 118.7, 120.9, 120.9, 121.0, 121.0, 121.5, 124.2, 124.5, 125.9, 126.2, 126.5, 126.9, 131.6, 138.3, 147.5, 149.2, 153.1, 155.2, 157.2; HRMS Calcd for $\text{C}_{17}\text{H}_{12}\text{Cl}_2\text{F}_3\text{N}_3\text{O}_2$ (M+H): 418.0337. Found: 418.0340. Yield: 86%.

6.2.8. 2-Chloro-6,7-dimethoxy-*N*-(4-phenoxyphenyl)quinazolin-4-amine (7)

^1H NMR (400 MHz, $\text{DMSO}-d_6$): δ 3.91 (s, 3H), 3.94 (s, 3H), 7.03 (d, J = 8.6 Hz, 2H), 7.07 (d, J = 8.8 Hz, 2H), 7.11–7.16 (m, 2H), 7.40 (t, J = 6.0 Hz, 2H), 7.71 (d, J = 8.8 Hz, 2H), 7.90 (s, 1H), 9.93 (s, 1H); ^{13}C NMR (100 MHz, $\text{DMSO}-d_6$): δ 56.5, 57.0, 103.4, 105.9, 107.5, 118.8, 119.5, 123.8, 125.3, 130.5, 134.3, 146.9, 149.5, 153.6, 153.9, 155.5, 157.4, 158.4; HRMS Calcd for $\text{C}_{22}\text{H}_{18}\text{ClN}_3\text{O}_3$ (M+H): 408.1115. Found: 408.1121. Yield: 55%.

6.2.9. 4-(2-Chloro-6,7-dimethoxyquinazolin-4-ylamino)-3-methylphenol (8)

^1H NMR (400 MHz, $\text{DMSO}-d_6$): δ 2.70 (s, 3H), 3.89 (s, 3H), 3.90 (s, 3H), 6.64 (d, J = 8.4 Hz, 1H), 6.71 (s, 1H), 7.04 (d, J = 8.4 Hz, 1H), 7.11 (s, 1H), 7.83 (s, 1H), 9.67 (s, 1H); ^{13}C NMR (100 MHz, $\text{DMSO}-d_6$): δ 18.5, 56.4, 56.5, 102.8, 107.0, 107.3, 113.5, 117.3, 128.0, 129.2, 136.7, 148.1, 149.2, 155.1, 155.5, 156.5, 160.1; HRMS Calcd for $\text{C}_{17}\text{H}_{16}\text{ClN}_3\text{O}_3$ (M+H): 346.0958. Found: 346.0951. Yield: 23%.

6.2.10. 4-(3-(2-Chloro-6,7-dimethoxyquinazolin-4-ylamino)phenoxy)benzonitrile (9)

^1H NMR (400 MHz, $\text{DMSO}-d_6$): δ 3.91 (s, 3H), 3.94 (s, 3H), 6.94 (d, J = 8.0 Hz, 1H), 7.17 (s, 1H), 7.21 (d, J = 8.8 Hz, 2H), 7.50 (t, J = 8.0 Hz, 1H), 7.65 (m, 2H), 7.86 (d, J = 8.8 Hz, 2H), 7.90 (s, 1H), 10.00 (s, 1H); ^{13}C NMR (100 MHz, $\text{DMSO}-d_6$): δ 56.0, 56.2, 102.1, 105.3, 106.6, 107.2, 113.8, 115.4, 118.4, 118.6, 118.7, 130.2,

134.6, 140.4, 148.2, 149.0, 153.9, 154.6, 155.0, 157.6, 160.7; HRMS Calcd for $C_{23}H_{17}ClN_4O_3$ (M - H): 431.0911. Found: 431.0909. Yield: 74%.

6.2.11. N-Benzyl-2-chloro-6,7-dimethoxyquinazolin-4-amine (10)

1H NMR (400 MHz, MeOH- d_4): δ 3.90 (s, 3H), 3.92 (s, 3H), 4.79 (s, 2H), 6.96 (s, 1H), 7.23 (t, J = 7.2 Hz, 1H), 7.31 (t, J = 7.2 Hz, 2H), 7.39 (d, J = 7.2 Hz, 2H), 7.47 (s, 1H); ^{13}C NMR (100 MHz, DMSO- d_6): δ 43.4, 55.8, 56.0, 102.2, 106.5, 106.8, 126.9, 127.4, 128.3, 138.9, 147.2, 148.5, 154.4, 155.0, 159.9; HRMS Calcd for $C_{17}H_{16}ClN_3O_2$ (M+H): 330.1009. Found: 330.1007. Yield: 21%.

6.3. General procedure for the synthesis of compounds 11–17

6.3.1. General procedure for the synthesis of compounds 11–17

To a solution of 2,4-dichloropyrimidine (1.0 mmol) and DIPEA (100 μ l) in isopropyl alcohol was added 0.7 mmol aniline derivatives and the mixtures stirred under ice-bath condition for 30 min. The resulting mixture was stirred at room temperature for 8 h. After the reaction was completed, the reaction mixture was washed with water, extracted with EtOAc, and the organic layer was dried over $MgSO_4$. After removal of $MgSO_4$ by filtration and evaporation of solvents, the crude residue was purified by chromatography on a silica gel column using MeOH/DCM as eluent (0% to 2%) to give compounds **11–17** (yield: 3–27%).

6.3.2. 2-Chloro-N-(3-ethynylphenyl)pyrimidin-4-amine (11)

1H NMR (400 MHz, MeOH- d_4): δ 3.48 (s, 1H), 6.66 (d, J = 6.0 Hz, 1H), 7.18 (d, J = 7.6 Hz, 1H), 7.30 (t, J = 7.6 Hz, 1H), 7.61 (d, J = 8.4 Hz, 1H), 7.72 (s, 1H), 8.05 (d, J = 6.0 Hz, 1H); ^{13}C NMR (100 MHz, $CDCl_3$): δ 78.6, 82.8, 102.9, 123.7, 123.9, 126.5, 129.8, 130.0, 137.5, 158.5, 161.1, 162.6; HRMS Calcd for $C_{12}H_8ClN_3$ (M+H): 230.0485. Found: 230.0478. Yield: 5%.

6.3.3. 2-Chloro-N-(3-chlorophenyl)pyrimidin-4-amine (12)

1H NMR (400 MHz, $CDCl_3$): δ 6.59 (d, J = 5.6 Hz, 1H), 7.18 (d, J = 8.0 Hz, 1H), 7.22 (d, J = 8.4 Hz, 1H), 7.31 (t, J = 8.0 Hz, 1H), 7.36 (s, 1H), 8.15 (d, J = 5.6 Hz, 1H); ^{13}C NMR (100 MHz, $CDCl_3$): δ 102.9, 120.6, 122.6, 125.8, 130.6, 135.2, 138.4, 158.2, 160.8, 162.0; HRMS Calcd for $C_{10}H_7Cl_2N_3$ (M+H): 240.0095. Found: 240.0101. Yield: 6%.

6.3.4. 2-Chloro-N-(4-chloro-3-(trifluoromethyl)phenyl)pyrimidin-4-amine (13)

1H NMR (400 MHz, $CDCl_3$): δ 6.55 (d, J = 5.6 Hz, 1H), 7.11 (s, 1H), 7.51 (d, J = 8.4 Hz, 1H), 7.63 (d, J = 8.4 Hz, 1H), 7.72 (s, 1H), 8.20 (d, J = 5.6 Hz, 1H); ^{13}C NMR (100 MHz, $CDCl_3$): δ 103.6, 120.8 (q), 123.7, 125.8, 128.1, 129.2, 129.5, 132.5, 136.2, 158.3, 160.9, 161.4; HRMS Calcd for $C_{11}H_6Cl_2F_3N_3$ (M+H): 307.9969. Found: 307.9969. Yield: 3%.

6.3.5. N-Benzyl-2-chloropyrimidin-4-amine (14)

1H NMR (400 MHz, MeOH- d_4): δ 4.55 (s, 2H), 6.60 (d, J = 5.2 Hz, 1H), 7.19–7.22 (m, 1H), 7.26–7.31 (m, 4H), 8.12 (d, J = 5.2 Hz, 1H); ^{13}C NMR (100 MHz, MeOH- d_4): δ 43.8, 104.4, 126.9, 127.4, 128.2, 138.3, 154.3, 160.2, 163.7; HRMS Calcd for $C_{11}H_{10}ClN_3$ (M+H): 220.0642. Found: 220.0640. Yield: 27%.

6.3.6. 2-Chloro-N-(4-phenoxyphenyl)pyrimidin-4-amine (15)

1H NMR (400 MHz, MeOH- d_4): δ 6.63 (d, J = 6.0 Hz, 1H), 6.96–7.00 (m, 4H), 7.08 (t, J = 7.2 Hz, 1H), 7.33 (t, J = 8.0 Hz, 2H), 7.54 (d, J = 8.0 Hz, 2H), 8.01 (d, J = 6.0 Hz, 1H); ^{13}C NMR (100 MHz, $CDCl_3$): δ 102.1, 119.0, 119.6, 123.7, 125.5, 129.8, 131.7, 155.6, 156.7, 158.0, 160.8, 163.0; HRMS Calcd for $C_{16}H_{12}ClN_3O$ (M–H): 296.0591. Found: 296.0583. Yield: 14%.

6.3.7. N^2,N^4 -Bis(3-ethynylphenyl)pyrimidine-2,4-diamine (16)

1H NMR (400 MHz, $CDCl_3$): δ 3.04 (s, 1H), 3.10 (s, 1H), 6.16 (d, J = 6.0 Hz, 1H), 7.13 (d, J = 8.0 Hz, 1H), 7.19–7.31 (m, 4H), 7.37 (d, J = 8.0 Hz, 1H), 7.45 (s, 1H), 7.54 (d, J = 8.4 Hz, 1H), 7.72 (s, 1H), 7.92 (br s, 1H), 8.06 (d, J = 6.0 Hz, 1H); ^{13}C NMR (100 MHz, $CDCl_3$): δ 77.0, 77.8, 83.0, 83.8, 97.2, 120.5, 122.4, 122.6, 123.0, 123.1, 125.2, 126.1, 128.0, 128.8, 129.3, 138.5, 139.7, 157.2, 159.8, 161.0; HRMS Calcd for $C_{20}H_{14}N_4$ (M+H): 311.1297. Found: 311.1291. Yield: 10%.

6.3.8. N^2,N^4 -Bis(4-chloro-3-(trifluoromethyl)phenyl)pyrimidine-2,4-diamine (17)

1H NMR (400 MHz, $CDCl_3$): δ 6.16 (d, J = 5.6 Hz, 1H), 6.60 (s, 1H), 7.10 (s, 1H), 7.38 (d, J = 8.4 Hz, 1H), 7.45 (d, J = 8.0 Hz, 1H), 7.60 (d, J = 8.4 Hz, 1H), 7.68 (d, J = 8.8 Hz, 1H), 7.72 (s, 1H), 7.92 (s, 1H), 8.12 (d, J = 5.6 Hz, 1H); ^{13}C NMR (100 MHz, MeOH- d_4): δ 99.6, 118.0 (q), 118.4 (q), 118.7, 118.9, 121.4, 121.6, 123.0, 123.3, 123.9, 124.1, 124.2, 124.3, 126.91–128.30 (m), 131.2, 131.4, 139.0, 139.6, 155.8, 159.1, 160.6; HRMS Calcd for $C_{18}H_{10}Cl_2F_6N_4$ (M+H): 467.0265. Found: 467.0254. Yield: 5%.

6.4. General procedure for synthesis of compounds 18 and 24

6.4.1. General procedure for synthesis of compounds 18–24

Aniline derivatives (0.5 mmol) were added to a solution of compound **1** (0.2 mmol) in isopropyl alcohol (3 ml), followed by the addition of a drop of concentrated HCl (100 μ l). The resulting solution was heated by using microwave irradiation to 150 °C for 30 min. After cooling, the mixture was filtered, and the solid was washed with isopropyl alcohol. The crude solid was dissolved in DCM and washed with saturated $NaHCO_3$ solution. The organic phase was dried over $MgSO_4$, filtered and concentrated under reduced pressure. The crude residue was purified by chromatography on a silica gel column using MeOH/DCM as eluent (0–5%) to give compounds **18–24** (yield: 20–80%).

6.4.2. N^2 -(4-Chloro-3-(trifluoromethyl)phenyl)- N^4 -(3-ethynylphenyl)-6,7-dimethoxy-quinazoline-2,4-diamine (18)

1H NMR (400 MHz, MeOH- d_4): δ 3.47 (s, 1H), 3.91 (s, 3H), 3.93 (s, 3H), 6.88 (s, 1H), 7.22 (d, J = 7.6 Hz, 2H), 7.31 (t, J = 8.0 Hz, 1H), 7.34 (d, J = 9.2 Hz, 1H), 7.53 (s, 1H), 7.80 (d, J = 8.0 Hz, 1H), 7.83 (s, 1H), 8.01–8.04 (m, 2H); ^{13}C NMR (100 MHz, MeOH- d_4): δ 54.9, 55.4, 77.1, 77.2, 83.1, 101.9, 105.0, 105.1, 117.1–117.2 (q), 121.5, 121.7, 121.9 (d), 122.5, 122.7, 122.9, 123.3, 124.4, 125.5, 126.9, 127.3, 127.6, 128.3, 128.5, 131.17, 139.5, 140.3, 147.0, 148.3, 155.1, 155.5, 157.8; HRMS Calcd for $C_{25}H_{18}ClF_3N_4O_2$ (M+H): 499.1149. Found: 499.1142. Yield: 33%.

6.4.3. N^4 -(3-Ethynylphenyl)-6,7-dimethoxy- N^2 -(4-phenoxyphenyl)quinazoline-2,4-diamine (19)

1H NMR (400 MHz, DMSO- d_6): δ 3.93 (s, 3H), 3.94 (s, 3H), 4.18 (s, 1H), 6.98 (d, 4H, J = 8.8 Hz), 7.13 (s, 1H), 7.15 (d, 1H, J = 7.6 Hz), 7.33–7.45 (m, 6H), 7.69 (d, 1H, J = 7.6 Hz), 7.75 (s, 1H), 8.10 (s, 1H), 10.33 (s, 1H), 10.90 (s, 1H); ^{13}C NMR (100 MHz, $CDCl_3$): δ 56.1, 56.2, 77.6, 83.2, 100.0, 104.4, 106.3, 117.9, 120.0, 120.8, 122.4, 122.5, 122.7, 125.2, 127.7, 128.8, 129.5, 135.9, 138.6, 146.7, 149.2, 151.3, 155.1, 155.9, 156.9, 158.2; HRMS Calcd for $C_{30}H_{24}N_4O_3$ (M+H): 489.1927. Found: 489.1925. Yield: 40%.

6.4.4. N^2 -(3-Chlorophenyl)- N^4 -(3-ethynylphenyl)-6,7-dimethoxyquinazoline-2,4-diamine (20)

1H NMR (400 MHz, MeOH- d_4): δ 3.47 (s, 1H), 3.93 (s, 3H), 3.94 (s, 3H), 6.88 (d, J = 8.0 Hz, 1H), 6.92 (s, 1H), 7.17 (t, J = 8.0 Hz, 1H), 7.22 (d, J = 7.6 Hz, 1H), 7.34 (t, J = 8.0 Hz, 1H), 7.53 (d, J = 8.4 Hz, 1H), 7.58 (s, 1H), 7.80 (s, 2H), 7.87 (d, J = 8.4 Hz, 1H); ^{13}C NMR (100 MHz, MeOH- d_4): δ 54.9, 55.4, 77.1, 83.1, 102.0,

104.9, 104.9, 117.0, 118.4, 120.5, 122.6, 123.0, 125.5, 126.9, 128.5, 129.3, 133.7, 139.6, 142.3, 146.9, 148.5, 155.1, 155.8, 157.9; HRMS Calcd for $C_{24}H_{19}ClN_4O_2$ (M+H): 431.1275. Found: 431.1280. Yield: 34%.

6.4.5. N^4 -(3-Ethynylphenyl)- N^2 -(2-fluoro-5-methylphenyl)-6,7-dimethoxyquinazoline-2,4-diamine (21)

1H NMR (400 MHz, MeOH- d_4): δ 2.18 (s, 3H), 3.45 (s, 1H), 3.95 (s, 3H), 3.96 (s, 3H), 6.75 (br s, 1H), 6.91–6.98 (m, 2H), 7.23 (d, J = 7.6 Hz, 1H), 7.31 (t, J = 8.0 Hz, 1H), 7.62 (s, 1H), 7.75–7.77 (m, 2H), 7.91 (d, J = 7.6 Hz, 1H); ^{13}C NMR (100 MHz, $CDCl_3$): δ 21.2, 56.1, 56.1, 75.5, 100.3, 104.4, 105.5, 114.0, 114.2, 121.4, 122.2, 122.3, 122.7, 122.7, 125.3, 127.6, 127.7, 127.8, 128.9, 133.7, 133.7, 138.6, 146.9, 148.1, 149.7, 152.1, 155.2, 155.2, 157.1; HRMS Calcd for $C_{25}H_{21}FN_4O_2$ (M+H): 429.1727. Found: 429.1721. Yield: 20%.

6.4.6. N^2 -Benzyl- N^4 -(3-ethynylphenyl)-6,7-dimethoxyquinazoline-2,4-diamine (22)

1H NMR (400 MHz, DMSO- d_6): δ 3.84 (s, 3H), 3.85 (s, 3H), 4.15 (s, 1H), 4.53 (d, J = 6.4 Hz, 2H), 6.75 (s, 1H), 7.10–7.19 (m, 3H), 7.27 (t, J = 8.0 Hz, 1H), 7.28 (d, J = 7.2 Hz, 2H), 7.33 (d, J = 7.2 Hz, 2H), 7.63 (s, 1H), 7.90 (s, 1H), 9.14 (s, 1H); ^{13}C NMR (100 MHz, $CDCl_3$): δ 29.3, 45.2, 55.7, 55.9, 76.8, 83.0, 100.1, 103.4, 105.2, 121.6, 122.2, 124.2, 126.7, 126.9, 127.1, 128.1, 128.4, 138.5, 139.3, 145.7, 154.7, 156.5, 158.0; HRMS Calcd for $C_{25}H_{22}N_4O_2$ (M+H): 411.1821. Found: 411.1826. Yield: 15%.

6.4.7. 4-(3-(4-(3-Ethynylphenylamino)-6,7-dimethoxyquinazolin-2-ylamino)phenoxy)-benzonitrile (23)

1H NMR (400 MHz, $CDCl_3$): δ 3.05 (s, 1H), 3.93 (s, 3H), 3.95 (s, 3H), 6.61 (d, J = 7.6 Hz, 1H), 6.92 (s, 1H), 6.94 (s, 1H), 7.01 (d, J = 9.2 Hz, 2H), 7.20 (d, J = 7.6 Hz, 1H), 7.26 (t, J = 8.0 Hz, 2H), 7.35 (d, J = 7.2 Hz, 2H), 7.54 (d, J = 9.2 Hz, 2H), 7.64 (s, 1H), 7.66 (d, J = 8.0 Hz, 1H), 7.73 (s, 1H); ^{13}C NMR (100 MHz, $CDCl_3$): δ 56.1, 56.2, 77.6, 83.2, 100.1, 104.6, 105.3, 106.3, 110.5, 112.8, 115.2, 118.0, 119.0, 122.7, 122.8, 125.4, 127.9, 128.8, 130.1, 133.9, 138.5, 142.1, 147.0, 148.9, 155.1, 155.1, 155.3, 157.0, 161.6; HRMS Calcd for $C_{31}H_{23}N_5O_3$ (M+H): 514.1879. Found: 514.1888. Yield: 80%.

6.4.8. 4-(4-(4-(3-Ethynylphenylamino)-6,7-dimethoxyquinazolin-2-ylamino)phenoxy)-benzonitrile (24)

1H NMR (400 MHz, DMSO- d_6): δ 3.92 (s, 3H), 3.94 (s, 3H), 4.22 (s, 1H), 7.06 (d, J = 8.4 Hz, 2H), 7.10–7.15 (m, 3H), 7.36 (d, J = 7.6 Hz, 1H), 7.43 (t, J = 8.0 Hz, 1H), 7.53 (d, J = 7.6 Hz, 2H), 7.68 (d, J = 7.6 Hz, 1H), 7.74 (s, 1H), 7.85 (d, J = 8.4 Hz, 2H), 8.03 (s, 1H); ^{13}C NMR (100 MHz, $CDCl_3$): δ 56.1, 56.2, 77.6, 83.2, 100.2, 104.6, 105.0, 106.3, 117.3, 119.0, 120.6, 121.0, 122.6, 122.7, 125.5, 127.8, 128.8, 134.0, 137.6, 138.6, 146.8, 148.6, 149.2, 155.1, 155.7, 157.0, 162.4; HRMS Calcd for $C_{31}H_{23}N_5O_3$ (M+H): 514.1879. Found: 514.1876. Yield: 75%.

6.5. Biological assays

6.5.1. Cell culture

SK-Hep-1, PC9 cells were maintained in DMEM supplemented with 10% FBS, 100 units/mL penicillin G, 100 μ g/mL streptomycin sulfate and 25 μ g/mL amphotericin B in a 37 °C humidified incubator in an atmosphere of 5% CO_2 in air.

6.5.2. Western blot

SK-Hep-1 and PC9 cells (3×10^5 cells) were treated with compounds at various doses in 60 mm dish. 40 μ g/per lane of cell lysates were analyzed by western blot. Antibodies for immunoblotting such as anti-Akt1 and CIP2A were purchased from Santa Cruz Biotechnology (San Diego, CA). Other antibodies such as

EGFR, p-EGFR, PARP and p-Akt (Ser473) were from Cell Signaling (Danvers, MA).

6.5.3. Cell death detection ELISA

The effect of compounds **4**, **19** and **22** on cell viability was assessed by a cell death detection ELISA kit (Roche Applied Science, Mannheim, Germany). SK-Hep-1 cells were treated with compounds **4** and **19** at **22** at 2.5 and 5 μ M for 24 h. The cells were collected and assayed according to the standard protocol provided by the manufacturer.

6.5.4. Apoptosis analysis

The apoptotic cells were assessed by flow cytometry (sub-G1). After Sk-Hep-1 cells were treated with compounds **4**, **19**, and **22**, cells were trypsinized, collected by centrifugation and resuspended in PBS. After centrifugation, the cells were washed in PBS and resuspended in propidium iodide (PI) staining solution. (Specimens were incubated in the dark for 30 min at 37 °C and then analyzed with an EPICS Profile II flow cytometer (Coulter Corp., Hialeah, FL). All experiments were performed in triplicate

6.5.5. MTT assay

The effect of individual test agents on cell viability was assessed by using the 3-(4,5-dimethylthiazol-2-yl)-2,5-diphenyltetrazolium bromide (MTT) assay in 6 replicates. SK-Hep-1 cells were seeded and incubated in 96-well, flat-bottomed plates in for 24 hours and were exposed to various concentrations of test agents dissolved in DMSO (final concentration, 0.1%) for 48 h. Controls received DMSO vehicle at a concentration equal to that in drug-treated cells. The medium was removed, replaced by 200 μ L of 0.5 mg/mL MTT in 10% fetal bovine serum containing DMEM, and cells were incubated in the carbon dioxide incubator at 37 °C for 2 h. Supernatants were removed from the wells and the reduced MTT dye was solubilized in 100 μ L/well DMSO. Absorbance at 570 nm was determined on a plate reader.

6.5.6. Quantitative real time polymerase chain reaction (qPCR) assay

Total RNA was isolated from SK-Hep1 cell line with TRIzol (Invitrogen). An aliquot of 2.5 μ g/12.1 μ L of total RNA was used as the template in the synthesis of first-strand cDNA using an oligo(dT) primer and the AMV reverse transcriptase system (Roche Diagnostics) by Thermal Cycler (RTC-200, MJ Reaserch). The method of qPCR was followed according to the method described by Ponchel et al.²³ qPCR was performed using a Roche LightCycler 480 sequence detection system (RocheApplied Science,). Thermocycling was performed in a final volume of 20 μ L containing 2.5 μ L of cDNA sample, 200 nM of each of the primers, and 6.5 μ L of SYBR Green I master mix (Roche). The relative differences in expression levels between genes were expressed using cycle time (Ct) values as follows: the Ct value of the gene of CIP2A was first normalized to that for GAPDH in the same sample, then the difference between the treatment and control group was calculated and expressed as an increase or decrease in cycle numbers compared with the control. Oligonucleotide sequences were as follows: CIP2A, 5'-TGG CAA GAT TGA CCT GGG ATT TGG A-3'(sense) and 5'-AGG AGT AAT CAA ACG TGG GTC CTG A-3'(antisense); GAPDH, 5'-CGA CCA CTT TGT CAA GCT CA-3'(sense) and 5'-AGG GGT CTA CAT GGC AAC TG-3'(antisense). The following PCR conditions were used: denaturation at 95 °C for 10 min followed by 40 cycles of 94 °C for 1 min, annealing for 1 min at 60 °C, and elongation for 1 min at 72 °C, and a final elongation step at 72 °C for 10 min.

6.5.7. Clonogenic assay

For colony formation, SK-Hep1 cells transfected with scramble siRNA or CIP2A-specific siRNA were seeded in triplicate onto

6 cm plates (10,000 cells per plate). After 7 days of culturing, cells were stained with crystal violet and colony containing more than 50 cells were counted.

Acknowledgments

We thank the National Science Council, Taiwan (NSC98-2320-B-010-005-My3 and NSC-100-2325-B-010-007) and National Yang Ming University, Taiwan for financial support. C.W.S. also thanks the National Research Institute of Chinese Medicine for NMR support.

Supplementary data

Supplementary data associated with this article can be found, in the online version, at <http://dx.doi.org/10.1016/j.bmc.2012.08.039>.

References and notes

- Chen, K. F.; Yu, H. C.; Liu, C. Y.; Chen, H. J.; Chen, Y. C.; Hou, D. R.; Chen, P. J.; Cheng, A. L. *Mol. Cancer Ther.* **2011**, *10*, 892.
- Wang, J.; Li, W.; Li, L.; Yu, X.; Jia, J.; Chen, C. *Int. J. Lab. Hematol.* **2011**, *33*, 290.
- Vaarala, M. H.; Vaisanen, M. R.; Ristimäki, A. *J. Exp. Clin. Cancer Res.* **2010**, *29*, 136.
- Dong, Q. Z.; Wang, Y.; Dong, X. J.; Li, Z. X.; Tang, Z. P.; Cui, Q. Z.; Wang, E. H. *Ann. Surg. Oncol.* **2010**, *18*, 857.
- Chen, K. F.; Liu, C. Y.; Lin, Y. C.; Yu, H. C.; Liu, T. H.; Hou, D. R.; Chen, P. J.; Cheng, A. L. *Oncogene* **2010**, *29*, 6257.
- Come, C.; Laine, A.; Chanrion, M.; Edgren, H.; Mattila, E.; Liu, X.; Jonkers, J.; Ivaska, J.; Isola, J.; Darbon, J. M.; Kallioniemi, O.; Thezenas, S.; Westermarck, J. *Clin. Cancer Res.* **2009**, *15*, 5092.
- Junttila, M. R.; Puustinen, P.; Niemela, M.; Ahola, R.; Arnold, H.; Bottzauw, T.; Ala-aho, R.; Nielsen, C.; Ivaska, J.; Taya, Y.; Lu, S. L.; Lin, S.; Chan, E. K.; Wang, X. J.; Grenman, R.; Kast, J.; Kallunki, T.; Sears, R.; Kahari, V. M.; Westermarck, J. *Cell* **2007**, *130*, 51.
- Bielski, V. A.; Mumby, M. C. *Exp. Cell Res.* **2007**, *313*, 3117.
- Van Muijlwijk-Koezen, J. E.; Timmerman, H.; Van der Goot, H.; Menge, W. M.; Frijtag Von Drabbe Kunzel, J.; De Groote, M.; IJzerman, A. P. *J. Med. Chem.* **2000**, *43*, 2227.
- Liu, F.; Chen, X.; Allali-Hassani, A.; Quinn, A. M.; Wigle, T. J.; Wasney, G. A.; Dong, A.; Senisterra, G.; Chau, I.; Siarheyeva, A.; Norris, J. L.; Kireev, D. B.; Jadhav, A.; Herold, J. M.; Janzen, W. P.; Arrowsmith, C. H.; Frye, S. V.; Brown, P. J.; Simeonov, A.; Vedadi, M.; Jin, J. *J. Med. Chem.* **2010**, *53*, 5844.
- Hattori, K.; Kido, Y.; Yamamoto, H.; Ishida, J.; Kamijo, K.; Murano, K.; Ohkubo, M.; Kinoshita, T.; Iwashita, A.; Mihara, K.; Yamazaki, S.; Matsuoka, N.; Teramura, Y.; Miyake, H. *J. Med. Chem.* **2004**, *47*, 4151.
- Wagner, J.; von Matt, P.; Sedrani, R.; Albert, R.; Cooke, N.; Ehrhardt, C.; Geiser, M.; Rummel, G.; Stark, W.; Strauss, A.; Cowan-Jacob, S. W.; Beerli, C.; Weckbecker, G.; Evenou, J. P.; Zenke, G.; Cottens, S. *J. Med. Chem.* **2009**, *52*, 6193.
- Smits, R. A.; Adami, M.; Istyastono, E. P.; Zuiderveld, O. P.; van Dam, C. M.; de Kanter, F. J.; Jongejan, A.; Coruzzi, G.; Leurs, R.; de Esch, I. J. *J. Med. Chem.* **2010**, *53*, 2390.
- Hennequin, L. F.; Boyle, F. T.; Wardleworth, J. M.; Marsham, P. R.; Kimbell, R.; Jackman, A. L. *J. Med. Chem.* **1996**, *39*, 695.
- Shreder, K. R.; Wong, M. S.; Nomanbhoy, T.; Leventhal, P. S.; Fuller, S. R. *Org. Lett.* **2004**, *6*, 3715.
- Chilin, A.; Conconi, M. T.; Marzaro, G.; Guiotto, A.; Urbani, L.; Tonus, F.; Parnigotto, P. *J. Med. Chem.* **1996**, *39*, 695.
- Smaill, J. B.; Palmer, B. D.; Rewcastle, G. W.; Denny, W. A.; McNamara, D. J.; Dobrusin, E. M.; Bridges, A. J.; Zhou, H.; Showalter, H. D.; Winters, R. T.; Leopold, W. R.; Fry, D. W.; Nelson, J. M.; Slinkak, V.; Elliot, W. L.; Roberts, B. J.; Vincent, P. W.; Patmore, S. J. *J. Med. Chem.* **1993**, *36*, 42.
- Bridges, A. J.; Zhou, H.; Cody, D. R.; Rewcastle, G. W.; McMichael, A.; Showalter, H. D.; Fry, D. W.; Kraker, A. J.; Denny, W. A. *J. Med. Chem.* **1996**, *39*, 267.
- Morphy, R. *J. Med. Chem.* **2010**, *53*, 1413.
- Cai, X.; Zhai, H. X.; Wang, J.; Forrester, J.; Qu, H.; Yin, L.; Lai, C. J.; Bao, R.; Qian, C. *J. Med. Chem.* **2000**, *43*, 53.
- Chen, K. F.; Tai, W. T.; Huang, J. W.; Hsu, C. Y.; Chen, W. L.; Cheng, A. L.; Chen, P. J.; Shiau, C. W. *Eur. J. Med. Chem.* **2011**, *46*, 2845.
- Sirisoma, N.; Kasibhatla, S.; Pervin, A.; Zhang, H.; Jiang, S.; Willardsen, J. A.; Anderson, M. B.; Baichwal, V.; Mather, G. G.; Jessing, K.; Hussain, R.; Hoang, K.; Pleiman, C. M.; Tseng, B.; Drewe, J.; Cai, S. X. *J. Med. Chem.* **2008**, *51*, 4771.
- Ponchel, F.; Toomes, C.; Bransfield, K.; Leong, F. T.; Douglas, S. H.; Field, S. L.; Bell, S. M.; Combaret, V.; Puisieux, A.; Mighell, A. J.; Robinson, P. A.; Inglehearn, C. F.; Isaacs, J. D.; Markham, A. F. *BMC Biotechnol.* **2003**, *3*, 18.